— Original Paper —

Numerical predictions of sulfur and nitrogen depositions through fog in forest areas

Hikari Shimadera[1, 2], Akira Kondo[1], Akikazu Kaga[1], Kundan Lal Shrestha[1, 2], Yoshio Inoue[1]

[1] Graduate School of Engineering, Osaka University

Yamadaoka 2-1, Suita, Osaka, Japan 565-0871

[2] Research Fellow of the Japan Society for the Promotion of Science

This paper presented a method to estimate spatial distributions of fog water deposition and corresponding sulfur and nitrogen depositions. A two-dimensional fog deposition model (FDM) to predict turbulent fog water flux was developed. The FDM-predicted turbulent fog water flux depended on wind speed and parameters on forest. Comparisons of FDM with measurement data showed that the model well reproduced the turbulent deposition of fog water during typical fog events in mountainous regions. In order to estimate fog deposition in the Kinki Region of Japan, FDM was utilized with results derived from the 5th generation Mesoscale Model (MM5) and the Community Multiscale Air Quality model (CMAQ) in March 2005. In the mountainous areas, the ratios of fog water deposition to rainfall reached up to 22.5% (mean = 3.4 %). The amount of S and NO_Y deposition through fog was equivalent to that through rainfall and more than that through dry deposition in some areas. Longer term prediction (1year ~) is required for further study because the contribution of fog may considerably vary with seasonal variations in meteorology, air quality and vegetation structure.

Key words: Fog deposition model; Acid deposition, Forest; MM5/CMAQ

1. Introduction

Fog is a cloud on the ground surface and reduces the horizontal visibility to less than 1000 m. Fog can be classified into several types, such as radiation fog and mountain fog, in accordance with the formation mechanism. Radiation fog occurs through radiative cooling of humid air masses typically from night to early in the morning on flat terrains and in valleys. Mountain fog mainly occurs through orographic lifting of humid air masses and horizontal advection of low-level cloud to mountain ranges (Klemm et al., 2005).

Fog can affect forest ecosystems in mountainous areas, in which fog occurs more frequently than in other areas. Fog water deposition through the interception of fog droplets by vegetation can be an important part of the hydrologic budget of forests (Vong et al., 1991; Dawson, 1998). Ionic concentrations in fog water are much higher than those in rain water (Neal et al., 2003; Aikawa et al., 2006). Consequently, fog can contribute significantly to the deposition of ionic compounds in mountainous forest areas. The effects of fog may be more pronounced in Japan than in other countries because approximately two-thirds of the land area are covered with forests, most of which are located in mountainous regions.

The amounts of fog water deposition have been measured using a variety of approaches, such as the through fall measurement (Kobayashi et al., 2001) and the eddy covariance method (Burkard et al., 2003; Klemm et al., 2005). Numerical models also have been utilized to estimate fog water deposition. A one-dimensional model developed by Lovett (1984) has been widely used to predict turbulent deposition of fog in various mountain forests (Miller et al., 1993; Baumgardner et al., 2003). Katata et al. (2008) modified a one-dimensional land surface model called SOLVEG to better predict fog water deposition, and showed the modified SOLVEG agreed better with the measurement data by Klemm et al. (2005) than the model developed by Lovett (1984).

The study of fog on a spatial scale requires numerical simulations because few fog monitoring sites exist and fog is highly variable according to regions. Shimadera et al. (2008) applied the 5th generation Penn State University/ National Center for Atmospheric Research Mesoscale Model (MM5) (Grell et al. 1994) version 3.7 to fog simulation for months in the Kinki Region of Japan, and showed that the model well reproduced occurrence of fog. Shimadera et al. (2009) utilized the U.S. Environmental Protection Agency's Models-3 Community Multiscale Air Quality (CMAQ) modeling system (Byun and Ching, 1999) version 4.7 to estimate contribution of the transboundary transported air pollutants from the Asian

1 大阪大学大学院工学研究科 〒565-0871 大阪府吹田市山田丘 2-1

2 日本学術振興会特別研究員

Continent to fog chemistry in the Kinki Region of Japan. These previous studies made it possible to predict spatial distributions of fog occurrence and ionic concentrations in fog water. Because the deposition process of fog is not considered in the MM5/CMAQ modeling system, a numerical model to predict fog water deposition is required for an estimate of acid deposition through fog.

This paper describes a method to estimate spatial distributions of fog water deposition and corresponding acid deposition. A two-dimensional fog deposition model (FDM) to predict turbulent fog water flux was developed, and compared with the measurement data by Burkard et al. (2003) and Eugster et al. (2006). In order to estimate the spatial distribution of fog deposition in the Kinki Region of Japan, FDM was utilized with the results of MM5/CMAQ predictions by Shimadera et al. (2009).

2. Fog deposition model

2.1 Model structure

Equations to simulate turbulent airflow in and above a forest canopy are based on equations of mean motion and turbulence energy used by Yamada (1982). The horizontal wind direction is assumed to be constant in FDM. An equation of mean motion is

$$\frac{\partial u}{\partial t} = \frac{\partial}{\partial z}\left(K_M \frac{\partial u}{\partial z} \right) - C_d a_S(z) u|u|, \quad (1)$$

where u is the horizontal wind component (m s^{-1}), K_M is the eddy diffusivity of momentum (m^2 s^{-1}), C_d (= 0.2) is the drag coefficient for a forest canopy and $a_S(z)$ is the one-sided surface area density (m^2 m^{-3}), which is the sum of the leaf area density ($a_L(z)$) and the non-leaf area density. The vertical distribution of $a_S(z)$ within a canopy is obtained from a function proposed by Kondo and Arakashi (1976) as

$$a_S(z) = \frac{SAI}{h_{fc}} \hat{a}(Z) \quad \text{for} \quad 0 \le Z(= z/h_{fc}) \le 1, \quad (2)$$

$$\hat{a}(Z) = a_m \frac{1-Z}{1-Z_m} \exp\left[\frac{1}{2}(Z_m - \lambda)^2 - \frac{1}{2}(Z - \lambda)^2 \right], \quad (3)$$

$$Z_m \begin{cases} = \dfrac{\lambda + 1 - \sqrt{(\lambda - 1)^2 + 4}}{2} & \text{for} \quad \lambda > 1, \\ = 0 \quad \text{for} \quad \lambda \le 1, \end{cases} \quad (4)$$

$$\int_0^1 \hat{a}(Z) dZ = 1, \quad (5)$$

where SAI is the one-sided canopy surface area index (m^2 m^{-2}), which is the sum of the leaf area index (LAI) and the non-leaf area index ($NLAI$), and h_{fc} is the forest canopy height, λ is a parameter, Z_m is the height where $\hat{a}(Z)$ takes a maximum value, and a_m is a constant determined to satisfy Eq. (5).

An advection-diffusion equation of the liquid water content of fog (LWC) (kg m^{-3}) is

$$\frac{\partial LWC}{\partial t} = -u\frac{\partial LWC}{\partial x} - w\frac{\partial LWC}{\partial z} + \frac{\partial}{\partial z}\left(K_M \frac{\partial LWC}{\partial z} \right) - Dep. \quad (6)$$

The deposition term Dep is given by

$$Dep = f_L a_L(z) \varepsilon_{IM} |u| LWC, \quad (7)$$

where f_L is the portion of the effective leaf area for deposition of fog droplets and ε_{IM} is the impaction efficiency of fog droplet. According to Nagai (2002) and Katata et al. (2008), f_L and ε_{IM} can be expressed by

$$f_L = \frac{1 - \exp(-0.4 a_L(z)\Delta z)}{a_L(z)\Delta z}, \quad (8)$$

$$\varepsilon_{IM} = \left(\frac{\gamma St}{\gamma St + \alpha} \right)^{\beta}, \quad (9)$$

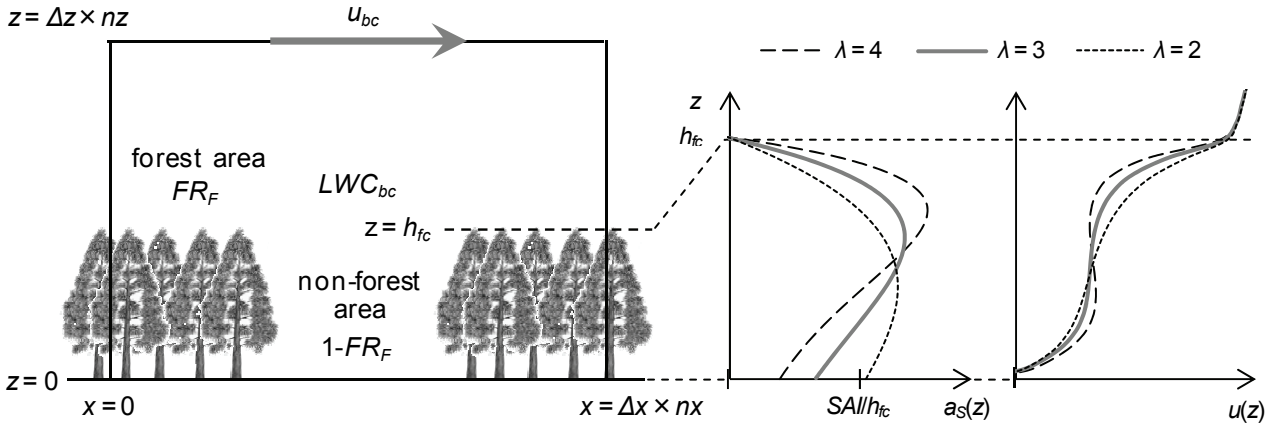

Fig. 1. Schematic diagram of FDM.

$$St = \frac{\rho_W d_p^2 |u|}{9 \mu_A d_L}, \quad (10)$$

where α, β and γ (= 5.0, 1.05 and 1 for needle leaf, and 0.5, 1.90 and 5 for broad leaf, respectively) are fitting parameters, St is the Stokes number, ρ_W is the density of water (kg m^{-3}), d_p (= $17.03LWC\times10^{-3}+9.72\times10^{-6}$) is the mean diameter of fog droplet (m), μ_A is the viscosity coefficient of air (kg m^{-1} s^{-1}), d_L (= 0.001 m for needle leaf and 0.030 m for broad leaf) is the characteristic leaf length (m).

Fig. 1 shows the schematic diagram of FDM, where u_{bc} is u at the upper boundary, LWC_{bc} is LWC above the forest canopy, FR_F is the fraction of the area covered with forests, nx and nz are the number of the horizontal and the vertical grids, respectively. Forests are allocated to the computational area from its horizontal edges according to FR_F. The vertical distribution patterns of a_S (z) and u within the forest canopy vary with the values of λ (the right side of Fig.1). FDM predicts steady state u and LWC for each simulation case. The following settings were used in every simulation cases in this study: Δx = 40 m, nx = 50, and $NLAI$ was assumed to be 0.5.

2.2 Features of the model

To show features of FDM, calculations were conducted with the following conditions: the atmosphere was neutral, u_{bc} = 0.5 ~ 10 m s^{-1}, LWC_{bc} = 0.0003 kg m^{-3}, h_{fc} = 18 m, LAI = 0.1 ~ 10, FR_F = 0.24 ~ 0.96, λ = 2 ~ 4, Δz = 1.5 m, nz = 30, and forest areas consisted of 100 % of needle-leaved trees.

Fig. 2 shows mean values of the fog water deposition velocity (V_{Dep} = fog water deposition flux/LWC_{bc}) in the computational area plotted against u_{bc} in the case of FR_F = 0.96, λ = 3. Since ε_{IM} increases with increasing u, V_{Dep} increases with increasing u_{bc}. When forest areas are thin, V_{Dep} considerably increases with an increase in LAI, i.e., an increase in available leaf area for fog deposition. As a forest becomes denser, drag force induced by the vegetation surface becomes larger, resulting in smaller u within a canopy. Therefore, when forest areas are dense, V_{Dep} does not very increase or can decrease with an increase in LAI.

Fig. 3 shows horizontal distributions of V_{Dep} in the cases of u_{bc} =10 m s^{-1}, LAI = 3, λ = 3. The largest V_{Dep} were observed at the windward edge of forest in every case. The values of V_{Dep} at the edge were 4.1, 2.3 and 1.5 times larger than those in the forest interiors in the cases of FR_F = 0.24, 0.48 and 0.96, respectively. Dry deposition at forest edges tend to be much larger than that in forest interiors (De Ridder et al., 2004). Such edge effects are also observed in fog water deposition (Kobayashi et al., 2001). Draaijers et al. (1994) indicated that edge effects were pronounced over a horizontal distance of approximately five times of the edge height. The results of FDM agreed with these findings.

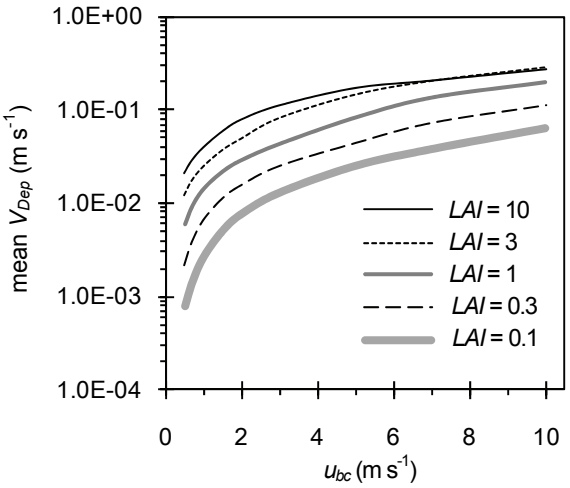

Fig. 2. Mean V_{Dep} in the computational area plotted against u_{bc} in the case of FR_F = 0.96, λ = 3.

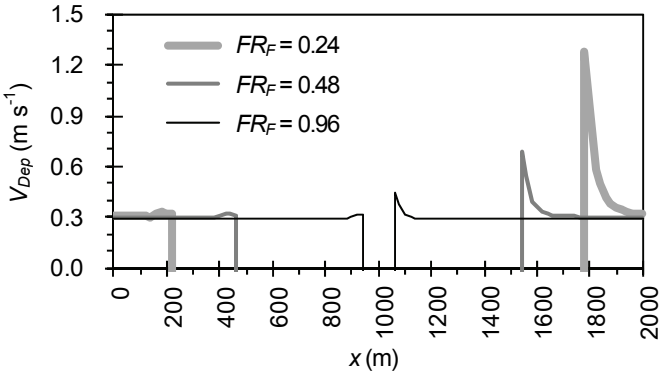

Fig. 3. Horizontal distribution of V_{Dep} in the computational area in the case of u_{bc} = 10 m s^{-1}, LAI = 3, λ = 3.

In the cases of λ = 2 and 4, the values of V_{dep} were generally smaller and larger by approximately 10% than those in the case of λ = 3. Due to the lack of data on vertical vegetation structure, λ was assumed to be 3 for the FDM applications described hereafter.

In the case that forest areas consisted of broad-leaved trees, the values of V_{dep} were smaller by approximately 20% than those in the case of needle-leaved trees. Further details about the effect of leaf shape on V_{Dep} are described in Katata et al. (2008).

2.3 Comparison with field measurement

Measurement data of fog water deposition with high temporal resolutions are preferable to the FDM evaluation. However, such measurement is not conducted in Japan. Therefore, measurement data of fog water deposition from Switzerland (Burkard et al., 2003) and Puerto Rico (Eugster et al., 2006) were utilized for the FDM evaluation.

Burkard et al. (2003) measured the turbulent fog water flux with the eddy covariance method at 45 m on a tower (15 m above the forest canopy) at a site (47°28′49″N, 8°21′05″E, 690 m above sea level) on the Lägeren mountain, approximately 15 km northwest of

Zurich, Switzerland. The vegetation cover around the site is mixed forest dominated by beech and Norway spruce. Fog water flux estimated by FDM was compared with the measurement for from September 2001 to March 2002. *LAI* around the site in the period was derived from the monthly datasets of the MODIS LAI product (available at http://cliveg.bu.edu/modismisr/index.html). The values of monthly *LAI* were ranged from 0.7 to 1.7. Calculations with FDM were conducted with the 30-minute measurement data and the following conditions: h_{fc} = 30 m, FR_F = 1, Δz = 1.5 m, nz = 30, and forest areas consisted of 50 % of needle-leaved trees and 50 % of broad-leaved trees.

Fig. 4 shows comparisons of FDM with the field measurement at the Lägeren site in Switzerland for accumulated turbulent fog water deposition and 30-minute V_{Dep} plotted against u_{bc}. While FDM-predicted V_{Dep} strongly depended on u_{bc}, measured V_{Dep} was hardly correlated with u_{bc}, particularly when u_{bc} was low. As a result, low correlation (r = 0.30) was observed between 30-minute turbulent fog water flux in FDM and in the measurement. The one-dimensional model developed by Lovett (1984) and the modified SOLVEG (Katata et al., 2008) should have difficulty in estimate of fog water deposition at the Lägeren site because the turbulent fog water flux in these models also depend on the horizontal wind speed. Radiation fog dominantly contributed to the turbulent fog water deposition at the Lägeren site (Burkard et al., 2003). Therefore, the discrepancies between FDM and the measurement were mainly attributed to uncertainties of the turbulent fog water deposition process during radiation fog events with low u_{bc}. Though FDM was not able to accurately reproduce the increase pattern of accumulated fog water deposition, the total fog water deposition in FDM agreed with that in the measurement.

Eugster et al. (2006) measured the turbulent fog water flux with the eddy covariance method at 7.25 m on a tower at a site (18°16′17″N, 65°45′39″W, 1015 m above sea level) in the Luquillo experimental forest in the northeastern part of Puerto Rico during 43 days between 26 June and 7 August 2002. The vegetation at the site consists of broad-leaved elfin cloud forest with the average canopy height of 2.5–3 m. The value of *LAI* derived from light extinction measurements was 2:1 ± 0.7 (Holwerda et al., 2006). Calculations

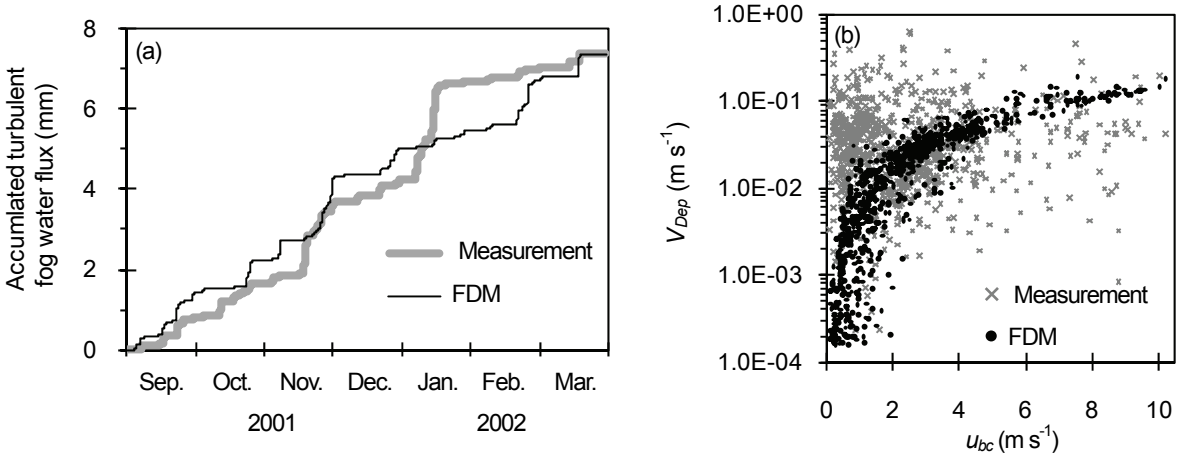

Fig. 4. Comparisons of FDM with the field measurement on the Lägeren mountain in Switzerland for (a) accumulated turbulent fog water flux and (b) V_{Dep} plotted against u_{bc} from September 2001 to March 2002.

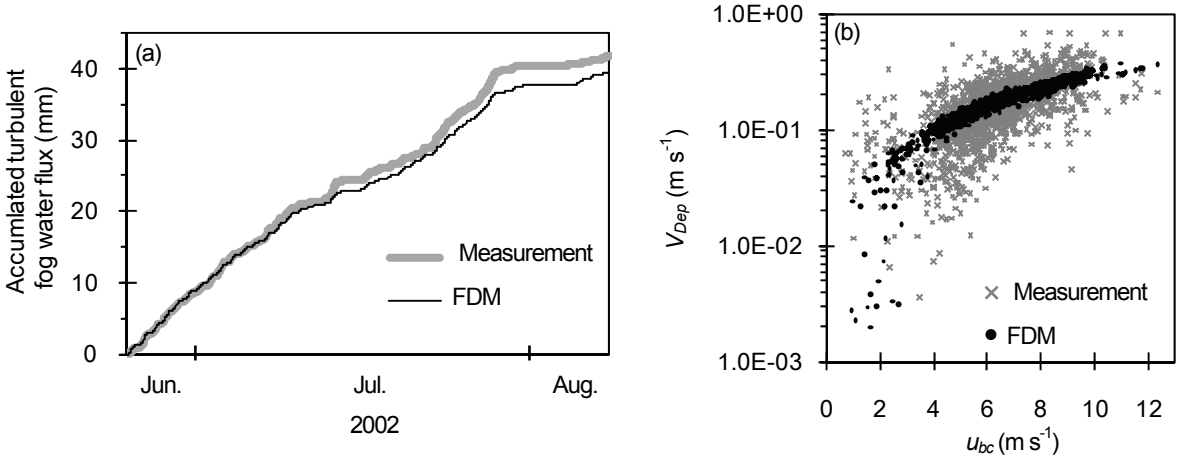

Fig. 5. Comparisons of FDM with the field measurement in the Luquillo experimental forest in Puerto Rico for (a) accumulated turbulent fog water flux and (b) V_{Dep} plotted against u_{bc} from 26 June to 7 August 2002.

with FDM were conducted with the 30-minute measurement data and the following conditions: h_{fc} = 3 m, LAI = 2.1, FR_F = 1, Δz = 0.5m, nz = 14, and forest areas consisted of 100 % of broad-leaved trees.

Fig. 5 shows comparisons of FDM with the field measurement at the Luquillo site in Puerto Rico for accumulated turbulent fog water deposition and 30-minute V_{Dep} plotted against u_{bc}. In contrast to the Lägeren site, relatively high u_{bc} was observed throughout the measurement period at the Luquillo site. Both FDM-predicted and measured V_{Dep} increased with increasing u_{bc}, which resulted in high correlation (r = 0.89) between 30-minute turbulent fog water flux in FDM and in the measurement. Consequently, FDM well reproduced the increase pattern of accumulated fog water deposition with slight underestimation. Katata et al. (2008) found that the fog water deposition velocity had high correlation with the horizontal wind speed over the forest canopy in both the modified SOLVEG and the measurement data at the Waldstein research site in Germany by Klemm et al. (2005). This finding agrees with the results of comparison of FDM with the measurement at the Luquillo site. mountain fog occurs very frequently at the Luquillo site due to the orographic lifting of humid air masses advected from the Atlantic Ocean by the northeasterly trade winds (Holwerda et al., 2006). The comparison of FDM with the measurement showed that FDM well reproduced the turbulent deposition of fog water during mountain fog events with relatively high u_{bc}.

The comparisons of FDM with the measurement data showed that FDM had difficulty in predictions during radiation fog events, but well predicted the turbulent fog water flux during mountain fog events. Because mountain fog occurs through advection of air masses, mountain fog events associate with higher wind speeds and more developed turbulent conditions than radiation fog events. In addition, mountain fog is the typical type of fog in mountainous regions (Klemm et al., 2005). These facts indicate that mountain fog is generally more important than radiation fog for the turbulent deposition of fog water onto mountainous forests. Therefore, FDM that captures the turbulent deposition of mountain fog is considered to be applicable to estimate of fog water deposition in mountainous regions.

3. Fog deposition in Kinki Region

3.1 Meteorology and air quality predictions

In order to estimate the spatial distributions of fog water deposition and corresponding acid deposition, FDM was utilized with the results of the MM5/CMAQ modeling system. MM5 is a three-dimensional, nonhydrostatic, terrain-following sigma-pressure coordinate model with a multiple-nest capability, several physics options, and a four-dimensional data assimilation capability. MM5 is widely used to drive air quality models. CMAQ is a three-dimensional Eulerian air quality modeling system that simulates the transport, transformation, and dry/wet deposition of various air pollutants and their precursors across spatial scales ranging from local to hemispheric. For our study, CMAQ was modified to output ionic concentrations in fog water.

The MM5/CMAQ modeling system was applied to the Kinki Region of Japan in March 2005 (Shimadera et al., 2009). Fig. 6 shows the modeling domains consisted of 4 domains from domain 1 (D1) covering a wide area of East Asia to domain 4 (D4) covering most of the Kinki Region. The horizontal resolutions and the number of grid cells in the domains are 54, 18, 6 and 2 km, and 105 × 81, 72 × 72, 99 × 99 and 126 × 126 for D1, domain 2 (D2), domain 3 (D3) and D4, respectively. The vertical layers consist of 24 sigma-pressure coordinated layers from the surface to 100 hPa with approximately 15, 50 and 110 m as the middle height of the first, second and third layer, respectively. The meteorology data and ionic concentration in fog water for FDM were derived from the lowest two layers.

Shimadera et al. (2009) compared the MM5/CMAQ predicted meteorology and SO_4^{2-}, NO_3^-, NH_4^+ concentrations in aerosol, rain

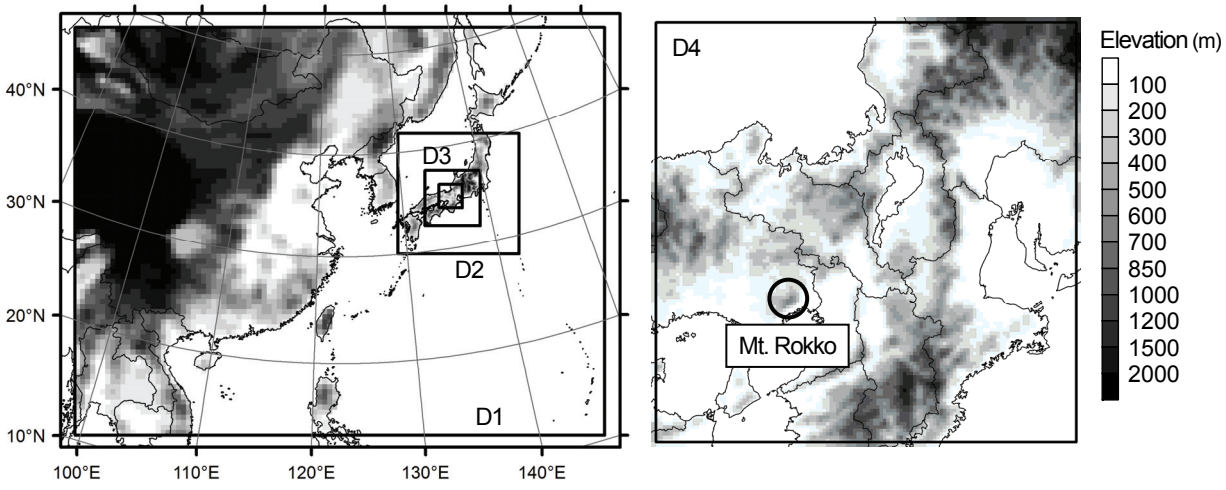

Fig. 6. Modeling domains for the meteorology and air quality predictions.

and fog with observation data obtained from meteorological observation by the Japan Meteorological Agency, fog sampling on Mt. Rokko by the Hyogo Prefectural Government, particulate matter sampling by the Osaka Prefectural Government, and acid deposition monitoring by the Ministry of the Environment (MOE) of Japan. The comparisons showed that the model well reproduced the meteorological fields and the long-range atmospheric transport of pollutants in the study region in March 2005. The model generally captured the occurrence of rainfall events and the total amount of rainfall. The model-predicted monthly mean concentrations of acidic compounds in rain were approximately within a factor of 2 of the observed data at the acid deposition monitoring sites in Japan. These findings indicated that the MM5/CMAQ could reasonably simulate acid depositions through rainfall. The model also approximately captured the occurrence of fog and the amount of acidic compounds in fog at Mt. Rokko fog sampling site. Therefore, the results of MM5/CMAQ predictions are applicable to estimate of acid deposition thorough fog. This finding and the comparisons of FDM with the field measurements indicate that estimate accuracy of acid deposition thorough fog by FDM with the results of MM5/CMAQ is probably not much worse than that of acid deposition thorough rainfall by MM5/CMAQ.

3.2 Forest data

Parameters on forest, such as FR_F and *LAI*, are important in FDM as shown in Fig. 2 and 3. For an application of FDM to D4, FR_F was obtained from the 100-m land use dataset of the Digital National Land Information (available at http://nlftp.mlit.go.jp/ksj/) prepared by the Ministry of Land, Infrastructure, Transport and Tourism in Japan. *LAI* was derived from the monthly 1-km dataset of the MODIS LAI product for March 2005. Forest classes, including deciduous needle-leaved forest (DNF), evergreen needle-leaved forest (ENF), deciduous broad-leaved forest (DBF) and evergreen broad-leaved forest (EBF) were determined by using the 1-km vegetation dataset of the 5th National Survey on the Natural Environment (available at http://www.biodic.go.jp/kiso/fnd_f.html) conducted by MOE of Japan.

Fig. 7 shows spatial distributions of FR_F, *LAI* and dominant forest class at each 2-km grid in D4. Forest areas account for 64.8 % of the land areas and 94.6 % of the mountainous areas (means areas with elevations > 500 m above sea level hereafter). DNF, ENF, DBF and EBF account for 0.3, 67.0, 28.5 and 4.2 % of the forest area, respectively. Because March is before or at the beginning of the vegetation growing season in D4, most of the forest areas tend to be thin. The north-eastern areas covered with DBF show the lowest *LAI* and the southern areas covered with ENF or EBF show relatively higher *LAI*. The values of *LAI* were less than 1, 2 and 3 in 22, 66 and 97% of forest areas.

3.3 Fog water deposition

The fog water deposition in D4 in March 2005 was estimated using FDM with the hourly results of MM5 predictions, the forest data described in 3.2, and the following conditions: h_{fc} = 18 m, Δz = 1.5 m, nz = 30.

Fig. 8 shows spatial distributions of model-predicted frequency of fog occurrence, fog water deposition and rainfall in D4 in March 2005. The fog frequency, fog water deposition and rainfall generally increased with increasing elevation. Mt. Rokko (Fig. 5) is characterized by its high frequency of fog (Aikawa et al., 2001). The values of fog frequency in large mountainous areas were comparable to or higher than that in Mt. Rokko. While the fog frequency and rainfall showed the highest values in the north-eastern area dominantly covered with DBF, the fog water deposition did not due to the thin vegetation cover. This trend may change in the vegetation growing season. In the mountainous areas, the amounts of fog water deposition ranged from 0 to 78.4 mm (mean = 9.3 mm), while rainfall ranged from 97.2 to 786 mm (mean = 273 mm). Consequently, the ratios of fog water deposition to rainfall at each 2-km grid reached up to 22.5% (mean = 3.4 %). Ratios of fog water deposition to rainfall in temperate mountainous forests in other literatures were 3.4 % at the Lägeren research site in Switzerland (Burkard et al., 2003), 9.4 % at the Waldstein research site in

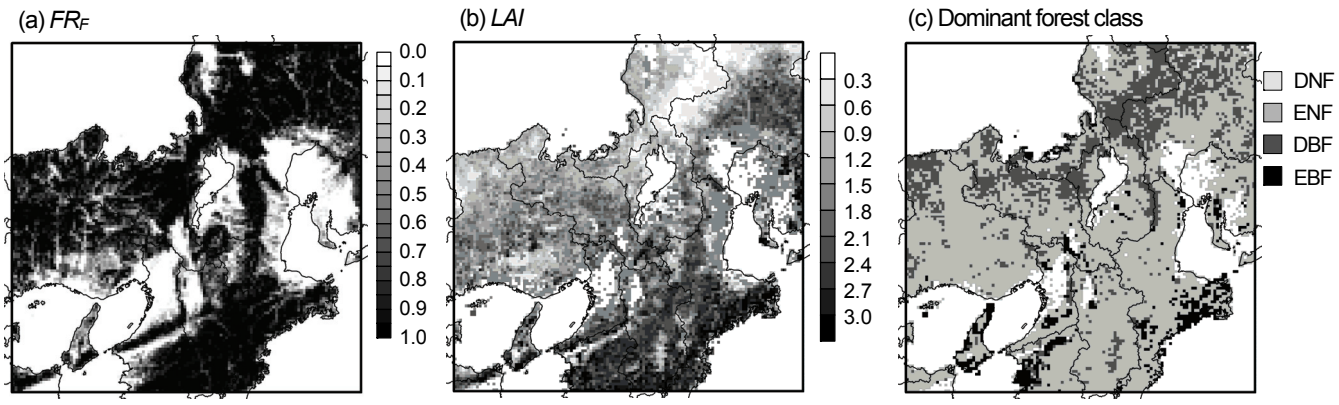

Fig. 7. Spatial distributions of (a) FR_F, (b) *LAI* and (c) dominant forest class in D4.

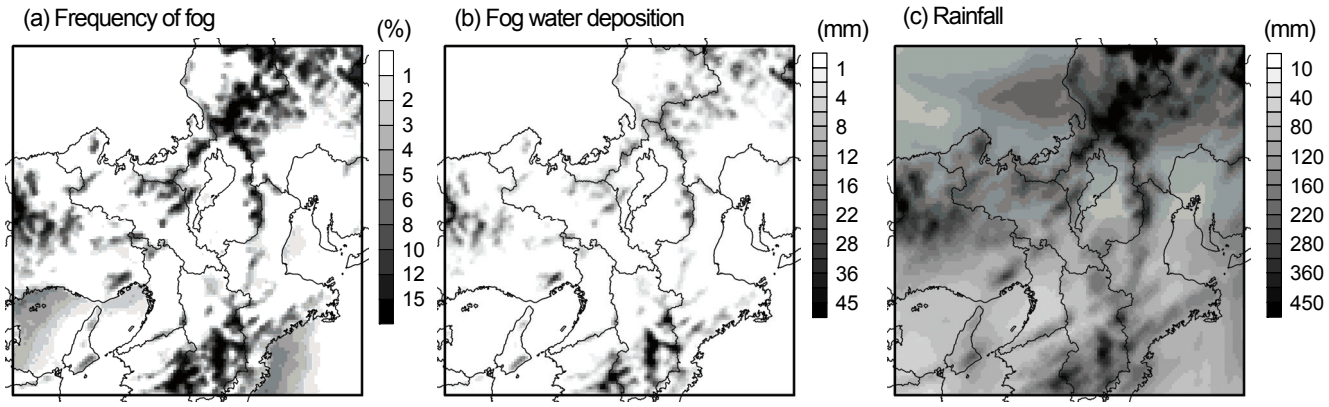

Fig. 8. Spatial distributions of predicted (a) frequency of fog, (b) fog water deposition and (c) rainfall in D4 in March 2005.

Germany (Klemm and Wrzesinsky, 2007), and 34 % at the coastal redwood forests in northern California (Dawson, 1998), respectively. The difference indicates that the ratios of fog water deposition to rainfall can considerably vary with changes in associated factors, such as fog frequency, amount of rainfall, wind speed, and vegetation structure. Therefore, the ratios of fog water deposition to rainfall in D4 can be change in the other seasons.

3.4 Acid deposition

Sulfur (S) and reactive nitrogen (NO_Y = NO + NO_2 + NO_3 + N_2O_5 + HNO_3 + HONO + aerosol nitrate in the present study) depositions through fog were estimated through multiplication of the FDM-predicted hourly fog water deposition flux by the CMAQ-predicted hourly concentration of acidic compounds in fog.

Fig. 9 shows spatial distributions of model-predicted S and NO_Y depositions through fog water deposition, rainfall and dry deposition in D4 in March 2005. Among the three deposition processes, rainfall contributed the most to S and NO_Y deposition in D4. In some areas, however, the amounts of S and NO_Y deposition through fog were equivalent to those through rainfall and larger than those through dry deposition. In the mountainous areas, the contribution ratios of S and NO_Y deposition through fog to the total deposition at each 2-km grid reached up to 27.4 % (mean = 4.6 %) and 37.6 % (mean = 4.8 %), respectively. The contribution of fog deposition can be larger in the vegetation growing season.

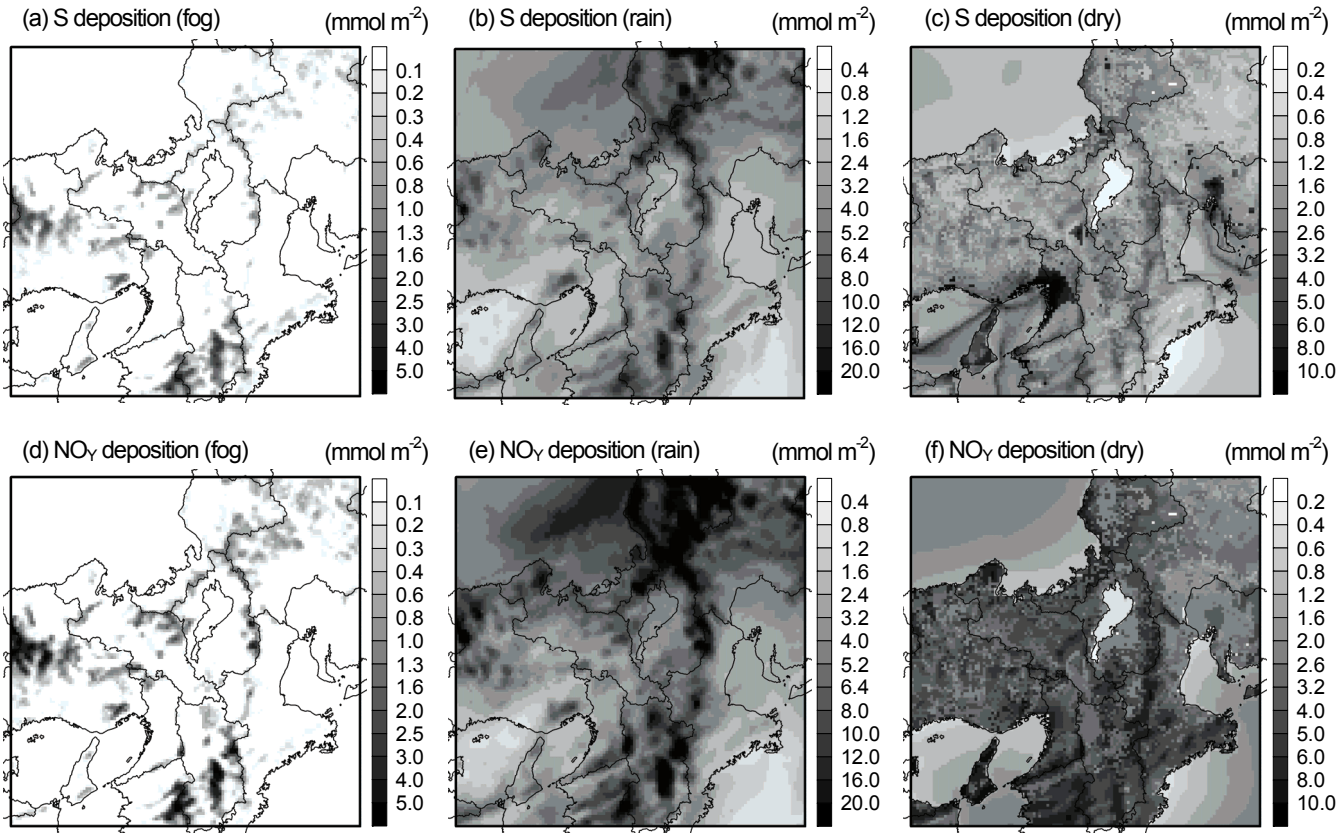

Fig. 9. Spatial distributions of predicted (a-c) S and (d-f) NO_Y depositions through fog, rain and dry depositions in D4 in March 2005.

4. Conclusion

This paper described a method to estimate the spatial distribution of fog water deposition and corresponding acid deposition by using the FDM and MM5/CMAQ modeling system.

FDM was developed to predict turbulent fog water flux in forest areas. The FDM-predicted fog water deposition velocity depended on wind speed and parameters on forest. In comparison of FDM with the measurement data at the Lägeren research site in Switzerland, FDM had difficulty in predictions of fog water deposition velocity due to uncertainties of the turbulent fog water deposition process during radiation fog events with low wind speed. However, the total amount of fog water deposition predicted by FDM agreed with the measurement at the Lägeren site. In comparison of FDM with the measurement data at the Luquillo experimental forest in Puerto Rico, FDM well reproduced the turbulent deposition of fog water during mountain fog events with relatively high wind speed. Because mountain fog is generally more important than radiation fog for the fog water deposition onto mountainous forests, FDM is considered to be applicable to estimate of fog water deposition in mountainous regions. Mechanisms of the turbulent fog water deposition during low wind speed periods should be further investigated for more reliable estimate of fog water deposition.

To estimate fog water deposition and corresponding S and NO_Y depositions, FDM was utilized with the results of MM5/CMAQ predictions in the Kinki Region of Japan in March 2005. In the mountainous areas, the ratios of fog water deposition to rainfall at each 2-km grid reached up to 22.5% (mean = 3.4 %). In some mountainous areas, the amount of S and NO_Y deposition through fog was equivalent to that through rainfall and more than that through dry deposition. The contribution of fog to acid deposition may considerably vary with seasonal variations in meteorology, air quality and vegetation structure. Therefore, long-term prediction (1year ~) is required for further study.

Acknowledgements

We are grateful to Werner Eugster for providing the measurement data at the Lägeren research site in Switzerland and the Luquillo experimental forest in Puerto Rico.

This work was supported by Grant-in-Aid for JSPS Fellows.

References

Aikawa, M., Hiraki, T., Shoga, M., Tamaki, M. (2001) Fog and precipitation chemistry at Mt. Rokko in Kobe, April 1997-March 1998. Water Air Soil Pollut., 130(1-4), 1517-1522.

Aikawa, M., Hiraki, T., Tamaki, M. (2006) Comparative field study on precipitation, throughfall, stemflow, fog water, and atmospheric aerosol and gases at urban and rural sites in Japan. Sci. Tot. Environ., 366 (1), 275-285.

Baumgardner, R.E., Kronmiller, K.G., Anderson, J.B., Bowser, J.J., Edgerton, E.S. (2003) Estimates of cloud water deposition at mountain acid deposition program sites in the Appalachian Mountains. Atmos, Environ., 33 (30), 5105-5114.

Burkard, R., Butzberger, P., Eugster, W. (2003) Vertical fogwater flux measurements above an elevated forest canopy at the Lägeren research site, Switzerland. Atmos. Environ., 37 (21), 2979-2990.

Byun, D.W., Ching, J.K.S. (1999) Science Algorithms of the EPA Models-3 Community Multi-scale Air Quality (CMAQ) Modeling System. NERL, Research Triangle Park, NC.

Dawson, T.E., (1998) Fog in the California redwood forest: Ecosystem inputs and use by plants. Oecol., 117 (4), 476-485.

De Ridder, K., Neirynck, J., Mensink, C. (2004) Parameterising forest edge deposition using effective roughness length. Agricultural and Forest Meteorology 123 (1-2), 1-11.

Draaijers, G.P.J., Van Ek, R., Bleuten, W. (1994) Atmospheric deposition in complex forest landscapes. Bound.-Lay. Meteorol., 69 (4), 343-366

Eugster, W., Burkard, R., Holwerda, F., Scatena, F.N., Bruijnzeel, L.A. (2006) Characteristics of fog and fogwater fluxes in a Puerto Rican elfin cloud forest. Agric. Forest Meteorol., 139 (3-4), 288-306.

Grell, G.A., Dudhia, J., Stauffer, D.R. (1994) A description of the fifth-generation Penn State/NCAR mesoscale model (MM5). NCAR Technical Note NCAR/TN-398+STR, 117 pp.

Holwerda, F., Burkard, R., Eugster, W., Scatena, F.N., Meesters, A.G.C.A., Bruijnzeel, L.A. (2006) Estimating fog deposition at a Puerto Rican elfin cloud forest site: Comparison of the water budget and eddy covariance methods. Hydrol. Process., 20 (13), 2669-2692

Katata, G., Nagai, H., Wrzesinsky, T., Klemm, O., Eugster, W., Burkard, R. (2008) Development of a land surface model including cloud water deposition on vegetation. J Appl. Meteorol. Climatol., 47 (8), 2129-2146.

Klemm, O., Wrzesinsky, T., Scheer, C. (2005) Fog water flux at a canopy top: Direct measurement versus one-dimensional model. Atmos. Environ., 39, 5375-5386.

Klemm, O., Wrzesinsky, T. (2007) Fog deposition fluxes of water and ions to a mountainous site in Central Europe. Tellus B, 59 (4), 705-714

Kobayashi, T., Nakagawa, Y., Tamaki, M., Hiraki, T., Aikawa, M. (2001) Cloud water deposition to forest canopies of Cryptomeria japonica at Mt. Rokko, Kobe, Japan. Water Air Soil Pollut., 130 (1-4 II), 601-606.

Kondo, J., Akashi, S. (1976) Numerical studies on the two-dimensional flow in horizontally homogeneous canopy

layers. Boundary-Layer Meteorol., 10 (3), 255-272.

Lovett, G.M. (1984) Rates and mechanisms of cloud water deposition to a subalpine balsam fir forest. Atmos. Environ.; 18, 361-371.

Miller, E.K., Panek, J.A., Friedland, A.J., Kadlecek, J., Mohnen, V.A. (1993) Atmospheric deposition to a high-elevation forest at Whiteface Mountain, New York, USA. Tellus , 45B: 209-227.

Nagai, H. (2002) Validation and sensitivity analysis of a new atmosphere-soil-vegetation model. J Appl. Meteorol., 41 (2), 160-176

Neal, C., Reynolds, B., Neal, M., Hill, L., Wickham, H., Pugh, B. (2003) Nitrogen in rainfall, cloud water, throughfall, stemflow, stream water and groundwater for the Plynlimon catchments of mid-Wales. Sci. Tot. Environ., 314-316, 121-151.

Shimadera, H., Shrestha, K.L., Kondo, A., Kaga, A., Inoue. Y. (2008) Fog simulation using a mesoscale model in and around the Yodo River Basin, Japan. J. Environ. Sci., 20 (7), 838-845.

Shimadera, H., Kondo, A., Kaga, A., Shrestha, K.L., Inoue, Y. (2009) Contribution of transboundary air pollution to ionic concentrations in fog in the Kinki Region of Japan. Atmos. Environ., 43 (37), 5894-5907.

Vong, R.J., Sigmon, J.T., Mueller, S.F. (1991) Cloud water deposition to appalachian forests. Environ. Sci. Technol. 25 (6), 1014-1021.

Yamada, T. (1982) A Numerical Model Study of Turbulent Airflow In and Above a Forest Canopy. J. Meteorol. Soc. Japan, 60, 439-454.

森林地域における霧による硫黄および窒素沈着量の数値予測

嶋寺　光，近藤　明，加賀　昭和，Shrestha Kundan Lal，井上　義雄

大阪大学大学院工学研究科

〒565-0871　大阪府吹田市山田丘　2-1

本論文では，霧水沈着による酸性物質沈着量の空間分布の予測手法を示した。まず，森林植生への霧水沈着を予測する数値モデルを開発し，霧水沈着モデルによる霧沈着速度は風速と森林植生密度に依存することを示した。また，霧水沈着モデルと観測データとの比較により，霧沈着モデルが山地における霧水沈着量を概ね再現できることを示した。霧沈着モデルとともに，数値気象/大気質モデル MM5/CMAQ による 2005 年 3 月の予測結果を用い，近畿地方における霧水沈着量とそれに伴う硫黄および窒素沈着量の空間分布を推定した。その結果，山地の森林地域における霧水沈着量と降雨量の比は最大 22.5%，平均 3.4%となった。硫黄および窒素沈着量については，霧による沈着量が，降雨による沈着量に匹敵し，乾性沈着による沈着量を上回る地域も見られた。酸性沈着における霧水沈着の寄与は，気象場，大気環境，植生構造の季節変動によって変化すると考えられるため，さらなる研究のためには，より長期間で予測を行う必要がある。